World Conference on Timber Engineering Oslo 2023

THE ADHESIVE SHEAR CONNECTION OF TIMBER AND CONCRETE SLABS IN HUMID ENVIRONMENT

Viktória Bajzecerová[1], Ján Kanócz[2], Viktor Karľa[3], Miroslava Javoríková[4]

ABSTRACT: The paper analyzes the influence of humidity and temperature changes on the normal and shear stresses in timber-concrete composite (TCC) panels with an adhesive shear connection. Three TCC panels were placed into an air-conditioned climate chamber and subjected to an environment typical of swimming-pool areas. Within the test, strains in two orthogonal directions were measured. A FEM model of the TCC specimens was created and validated against the measured strains. Using the FEM model, both normal and shear stresses were evaluated. The results show that the highest normal stresses occurred near the shear connection. In addition, increased timber moisture content by 2.1% caused achieving the flexural tensile strength of concrete perpendicular to the timber grain direction.

KEYWORDS: Timber-concrete composite slab, Adhesive shear connection, Hygrothermal load, shear stress

1 INTRODUCTION

Timber-concrete composites (TCC) are widely applied today as footbridge and/or bridge slabs [1,2], as well as the floor slabs of multi-story buildings [3,4]. For rapid construction, prefabricated TCC panels are especially useful, for which it is advantageous to use mass timber panels, such as vertically-laminated timber and cross-laminated timber plates [5–7]. There are numerous ways to ensure the concrete and timber layers' composite action, such as mechanical fasteners, notches, perforated steel strips, glued-in rods, and adhesives [8–11].

In comparison to mechanical fasteners, adhesive shear connections provide many advantages: rigid connection providing full interaction of timber and concrete slabs, a more uniform shear flow distribution, so no local stress concentrations occur, and a relatively simple calculation model since it is not necessary to consider the slip between timber and concrete parts of composite slab. While the glued-in rods method is well established and is becoming more common for the joining of timber structures, adhesive shear connections for TCC slabs still need to be studied in more detail from several aspects regarding its long-term behaviour, such as the creep, ageing of mechanical properties, as well as the effects of humidity, thermal changes and fire exposure [12].

The long-term bending tests of timber-concrete composite slabs with adhesive shear connection [13–15] showed that the adhesive might not be the weak link in their long-term behaviour. The composite action was unaffected by long-term loading. Results, however, indicated that the humidity and temperature conditions significantly impact the stress and deflection of the TCC over time. Furthermore, the effects of the ambient humidity and temperature changes are manifested increasingly with the growing rigidity of the shear connection between the timber and the concrete [16].

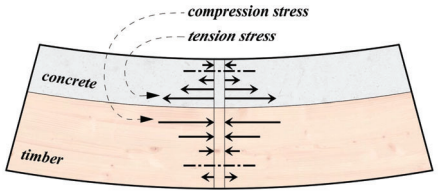

Figure 1: *The effect of restrained timber deformation in adhesively bonded TCC panel with increasing moisture content*

2 INFLUENCE OF HYGROTHERMAL LOAD

Due to uneven thermal and humidity deformations of concrete and timber in orthogonal directions, normal stress in composite members occurs, which can cause

[1] Viktória Bajzecerová, Technical University of Košice, Faculty of Civil Engineering, Košice, Slovak Republic. viktoria.bajzecerova@tuke.sk
[2] Ján Kanócz, Technical University of Košice, Faculty of Art, Slovak Republic. jan.kanocz@tuke.sk
[3] Viktor Karľa, Technical University of Košice, Faculty of Civil Engineering, Košice, Slovak Republic. viktor.karla@tuke.sk
[4] Miroslava Javoríková, Technical University of Košice, Faculty of Art, Slovak Republic. miroslava.javorikova@tuke.sk

https://doi.org/10.52202/069179-0419

defects of timber or concrete or the failure of the adhesive shear connection [17]. The effect of hygrothermal load on TCC is explained in Figure 1.

The increasing moisture content of the timber causes the elongation of the timber slab, which is limited by the adhesive concrete board and results in deflection and normal and shear stress near the glue line of TCC.

Using TCC panels as structural elements of roofs and walls of buildings with wellness, sauna or swimming pools may use the accumulation ability of the concrete and thus reduce the energy required for heating. On the other hand, the humid environment can cause unwanted deformations or possible failure of the glued joint. The presented study discusses the potential use of TCC with adhesive shear connection in such humid environmental conditions.

The research performed [19] dealt with the behaviour of TCC panels with an adhesive shear connection solely under the hygrothermal load and without other impacts, such as creep from gravity load or concrete shrinkage. The specimen loading was performed in a climate chamber. The test included temperature, moisture content, and strain measurements in two orthogonal directions. This paper presents evaluations of the measured results using the numerical FEM model. The aim was to analyse the normal and shear stresses caused by the humid environment typical of swimming-pool areas.

3 EXPERIMENTAL INVESTIGATION

3.1 SPECIMENS

Three specimens of TCC with adhesive shear connection were prepared to conduct the test (Figure 2).

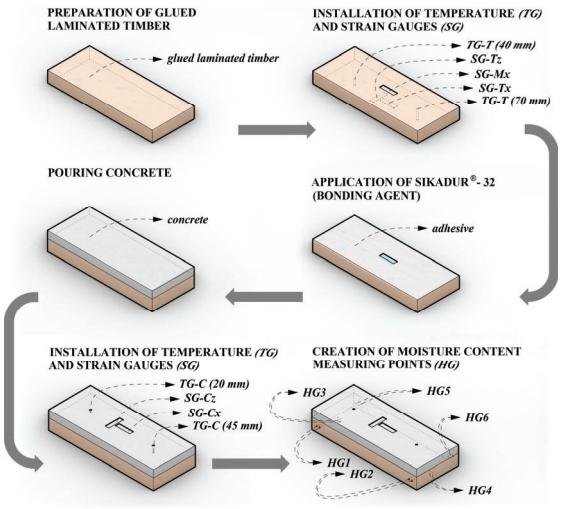

Figure 2: *Illustration of specimens' preparation*

First, strain gauges (SG) were installed on the top of the 750 mm long, 300 mm wide and 80 mm deep glued laminated timber slabs. After that, the 2-component epoxy adhesive Sikadur 32 was applied on top of the timber slabs. Subsequently, the 50 mm thick fresh concrete layer was cast on the wet adhesive on the timber slabs with no structural reinforcement. The prepared specimens were stored in lab conditions for about two years. Before the test, temperature (TG) and strain gauges (SG) were installed, as well as moisture content measure points (HG) were created. The final setup of specimens in the climate chamber is photographed in Figure 3, along with inset dimensions.

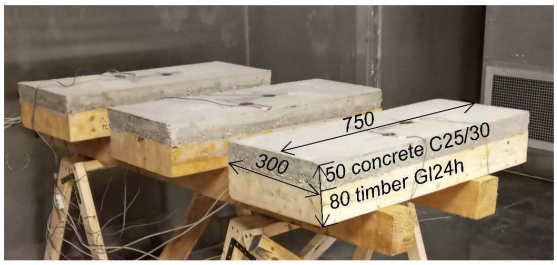

Figure 3: *Specimens in climate chamber; dimensions in mm*

3.2 MATERIAL PARAMETERS

For the test specimens, concrete C25/30 was chosen. Its real mechanical properties were defined according to EN standard 12390 [20]. Its cylinder and cube compressive strength 371 days after concreting were 55 MPa and 67 MPa, respectively. Its modulus of elasticity was determined as 26 GPa, flexural tensile strength as 8 MPa, and density as 2295 kg.m^{-3}. The mechanical parameters of the concrete are listed in Table 1.

Table 1: *Mechanical parameters of 371-day concrete*

Mechanical parameter	Value	Unit
Cylinder compressive strength	55	MPa
Cube compressive strength	67	MPa
Flexural tensile strength	8.1	MPa
Modulus of elasticity	26	GPa
Density	2295	kg.m^{-3}

The properties of glued laminated timber used for TCC panels were defined according to EN standard 408 [21]. Its modulus of elasticity parallel to the grain was determined as 13.9 GPa and bending strength as 50 MPa. The density of timber used was 425 kg.m^{-3}. The mechanical parameters of the timber are listed in Table 2.

Table 2: *Mechanical parameters of timber*

Mechanical parameter	Value	Unit
Bending strength	50.0	MPa
Modulus of elasticity parallel to the grain	13. 9	GPa
Density	425	kg/m^3

The modulus of elasticity and coefficient of thermal expansion of bonding agent Sikadur®-32, provided by the manufacturer [22], were 4.0 GPa, and 8.2x10^{-5} °C^{-1}, respectively. The shear strength of the adhesive connection with a value of 4.0 MPa was evaluated from 5 shear specimens of the same material used [7].

https://doi.org/10.52202/069179-0419

3.3 TES SET UP AND MEASURING METHODS

The three specimens (TC1, TC2 and TC3) were exposed to an environment with varying relative humidity and temperature by being placed in one chamber of air-conditioned climate chamber Thermotron WP-2(527)-2(THCM1-5) (Thermotron Industries, Holland, MI) (Figure 3).

Data acquisition system ALMEMO 5690-2 (Ahlborn, Holzkirchen, Germany) was used to store the data of ambient temperature, ambient relative humidity, and temperature gauges at various depths of the specimens (TG in Figure 2) at 15 min intervals.

Strain gauges with a length of 100 mm were placed in the x-direction and z-direction on top of the concrete and at the bottom of timber slabs (SG in Figure 2) to measure strains. Before concreting, another strain gauge was fixed on top of the timber slabs in the x-direction, which was 50 mm long (SG-Mx in Figure 2). Quantum MX 840 (HBM, Darmstadt, Germany) universal measurement amplifier module acquired data from strain gauges at 50 s intervals.

Moisture content in timber was monitored at six measuring points created on each specimen (HG in Figure 2) using a two-pins moisture content resistance meter WHT 770 (ELBEZ, Czech Republic).

3.4 HYGROTHERMAL LOAD

The hygrothermal load chosen for the analysis of humid conditions that are typical of that in swimming-pool areas are given in Table 3. The thermal and humidity conditions are similar to the measured data published in [18].

Table 3: *Considered environmental conditions*

Environment	T (°C)	RH (%)
0 - Initial conditions	20.0	65.0
1 – Swimming pool hall without mechanical ventilation	20.3	88.5
2 – Swimming pool hall with mechanical ventilation	34.3	51.8
3 - Shower room	34.6	71.9

T – temperature; RH – relative humidity

The initial conditions against which all further environmental changes were compared were a temperature (T) of 20°C and relative humidity (RH) of 65% (Environment 0). The initial conditions took 12 days, and the timber moisture content stabilised at 14%. The following environment settings were initiated only after stabilising the measured strains, the temperature in the whole depth of specimens and timber moisture content. Under humid Environment 1, warm and dry Environment 2, and warm Environment 3, the moisture content was stabilised at 16.1%, 11.4% and 14%, respectively.

3.5 THERMAL AND HUMIDITY EXPANSION COEFFICIENTS

Within the test, two segments of timber and concrete slab with dimensions of 300 mm × 450 mm were subjected to environmental changes. The same materials as for the TC specimen were used. Thermal and humidity expansion coefficients were calculated as the ratio of the measured strains and differences in temperature or moisture content of the timber slabs. These coefficients for concrete were calculated similarly, but the differences in relative humidity of the environment were used for the humidity expansion coefficient. More can be found in [19].

Table 4: *Thermal expansion Coefficients*

Thermal Expansion Coefficient	$\times 10^{-6}$ (1/°C)
Concrete	17.15
Timber parallel to grain	1.93
Timber perpendicular to grain	54.43

Table 5: *Humidity expansion Coefficients*

Humidity Expansion Coefficient	$\times 10^{-3}$ (-)
Concrete*	0.26
Timber parallel to grain	3.78
Timber perpendicular to grain	96.04

* *In relation to the change in RH (-)*

4 THEORETICAL INVESTIGATION

4.1 FEM MODEL GEOMETRY

The theoretical analysis of the specimens was performed by a finite element method (FEM) using ANSYS software [19]. The geometry of the model corresponded to real specimens. The depth of the adhesive layer was neglected, and the adhesive connection was defined as a bonded contact region between the timber and concrete. Regarding boundary conditions, zero displacements were set in 3 points, according to Figure 4. The mesh element size was set to 5 mm.

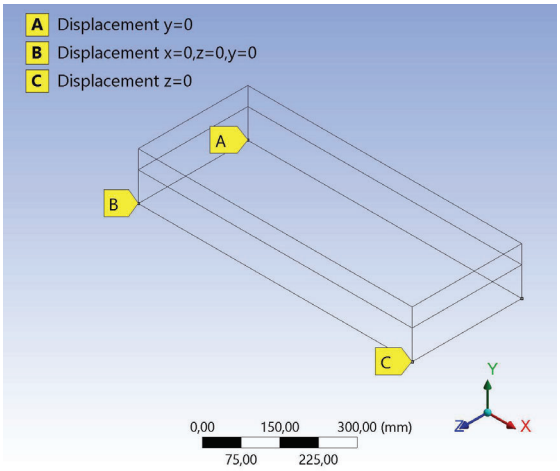

Figure 4: *FEM model – boundary conditions*

https://doi.org/10.52202/069179-0419

4.2 MATERIAL SETTINGS

The concrete was considered a linear elastic isotropic material. The mechanical parameters of the concrete were set according to Table 1. Poisson's ratio of concrete was assumed to be 0.18.
The timber was defined as linear elastic orthotropic material with the grain orientation in the x-axis, according to Figure 5.

Orthotropic Elasticity		
Young's Modulus X direction	13900	MPa
Young's Modulus Y direction	463	MPa
Young's Modulus Z direction	463	MPa
Poisson's Ratio XY	0	
Poisson's Ratio YZ	0	
Poisson's Ratio XZ	0	
Shear Modulus XY	690	MPa
Shear Modulus YZ	690	MPa
Shear Modulus XZ	69	MPa

Figure 5: *FEM model – the timber material parameters setting*

The reliable values of Poisson's ratios of timber were not possible to define due to a large discrepancy in available data [24]. Therefore, Poisson's ratios were set to zero because they were assumed to have a negligible effect on the results. A similar assumption was declared in [25].
Thermal and humidity expansion coefficients were set according to the measured values in Tables 4 and 5.

4.3 HYGROTHERMAL LOAD

In the FEM analysis, the temperature and humidity changes were modelled as a change in Thermal Conditions relative to the initial temperature.
Regarding the specimens' relatively small depth and the long duration of the hygrothermal load test step, it was assumed that the diffusion laws could be neglected. An instant adaptation of the temperature and humidity of both volumes of the FEM model was considered.

5 RESULTS

5.1 STRAINS

Strains parallel to the timber grain (x) and perpendicular to the timber grain (z) in the middle parts of the panels were analysed. The strain differences between each of the three environments (Table 3) and the initial environment were evaluated. In Figures 6 to 8, the strain differences over the cross-section of the TCC panel calculated from the measured (TC1, TC2, TC3) and calculated (FEM) data are plotted.
Although the calculation model did not consider the uneven temperature and humidity profiles in the cross-section and neglected the diffusion laws, it predicted the measured strains relatively well. Therefore, based on this comparison, the model was considered valid and suitable for the following analyses of normal and shear stresses.

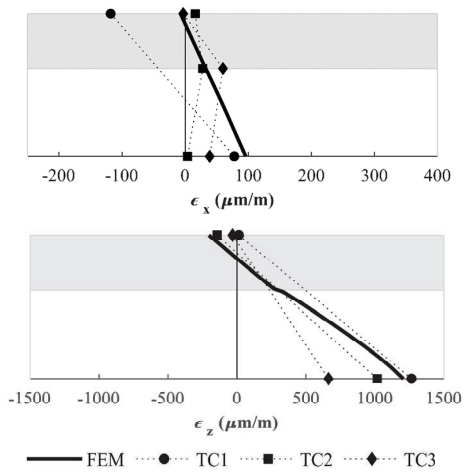

Figure 6: *Measured (TC1, TC2, TC3) and calculated (FEM) strains in x- (ε_x) and z- direction (ε_z) in Environment 1*

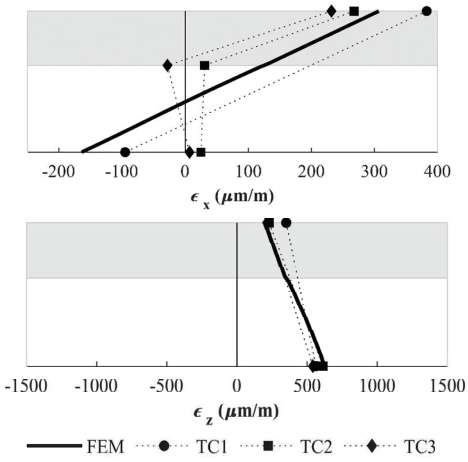

Figure 7: *Measured (TC1, TC2, TC3) and calculated (FEM) strains in x- (ε_x) and z- direction (ε_z) in Environment 2*

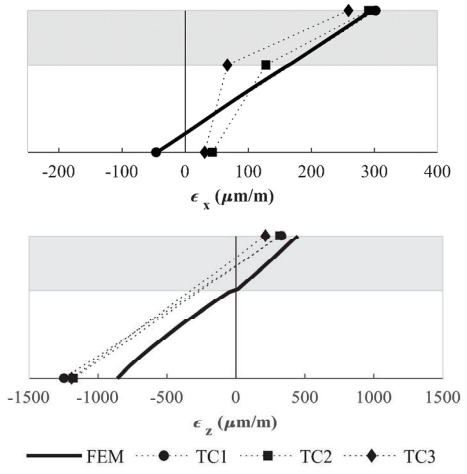

Figure 8: *Measured (TC1, TC2, TC3) and calculated (FEM) strains in x- (ε_x) and z- direction (ε_z) in Environment 3*

5.2 NORMAL STRESSES

Due to uneven and resisted deformation of the timber and concrete slab of the TCC panel, normal stresses occur (Figure 1). Therefore, the higher the differences in inelastic thermal and humidity strains, the higher stress can be expected. The normal stresses evaluated using FEM analysis are presented in Figures 9 to 13 and listed in Tables 6 and 7.

The tension in the concrete seems to be the weakest part of TCC slabs in humid Environment 1. The growth of the timber moisture content (MC) causes an increase in the tension stresses on the bottom surface of concrete up to +2.1 MPa in the x-direction (Figure 9), and in the z-direction increased almost to a value of the tensile strength of the concrete used with the value of +7.5 MPa (Figure 10). It should be noted that the tension strength of standard concrete is lower than that of the concrete used. The tension stresses usually bear the reinforcement in the concrete slabs, but the tension stress in the case of hygrothermal load occurs near the glued line and might cause the local failure of the adhesive connection.

The humid Environment 1 caused only a small increase in timber normal stresses with a value of less than 1 MPa.

The highest values of the normal stresses were expected in the middle part of the TCC slabs in both directions. Based on this expectation, the strain gauges were placed in the middle of the TCC slab span. However, as resulted from the FEM analysis of the warm Environment 3, the highest values of normal stresses were observed not in the middle part of the specimens, as previously expected in [19], but at the edges of specimens (Figures 13 and 14).

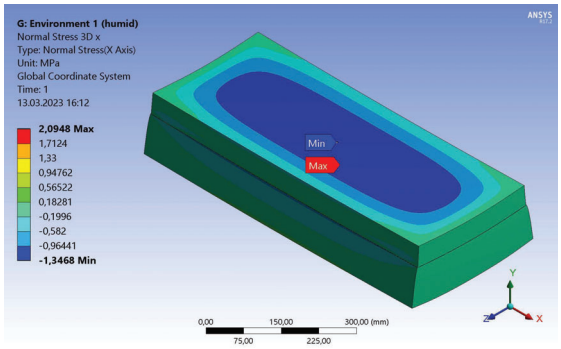

Figure 9: *Humid Environment 1 - normal stress in x direction*

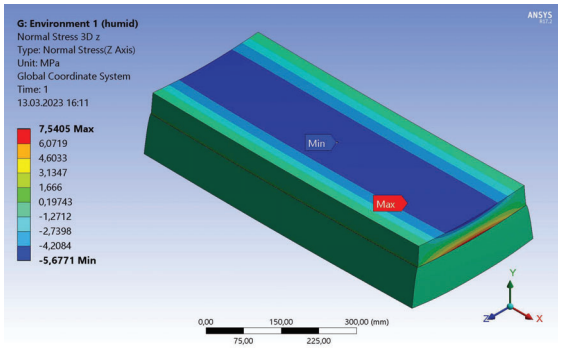

Figure 10: *Humid Environment 1 - normal stress in z direction*

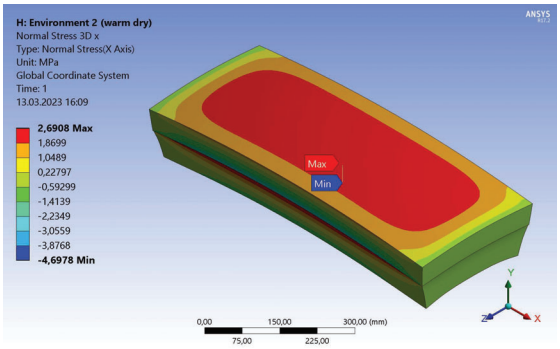

Figure 11: *Warm and dry Environment 2 - normal stress in x direction*

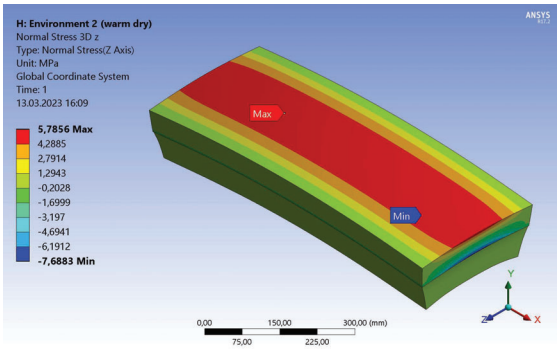

Figure 12: *Warm and dry Environment 2 - normal stress in z direction*

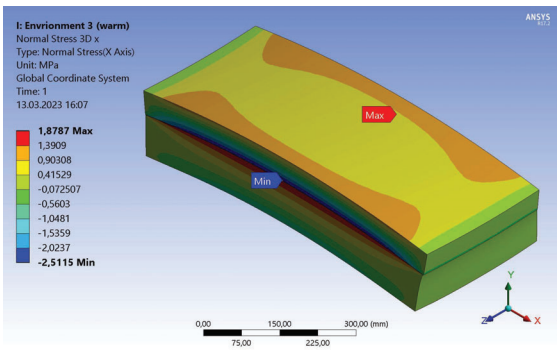

Figure 13: *Warm Environment 3 - normal stress in x direction*

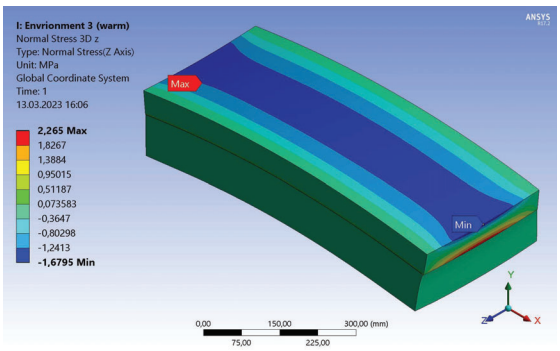

Figure 14: *Warm Environment 3 - normal stress in z direction*

https://doi.org/10.52202/069179-0419

The thermal expansion coefficient of concrete is almost 9-times higher than that of the timber parallel to the grain (in the x-direction), but on the contrary, it is 0.32-times lower than that of the timber perpendicular to the grain (in the z-direction). The orthotropic behaviour of the timber leads to a complex 2-dimensional problem of TCC slabs. From the Figure above, the highest stresses in all environments occurred solely in the concrete. Therefore, Tables 6 and 7 list the maximum stress values in timber and concrete parts separately.

Table 6: *Maximum values of normal stresses in x direction*

Env.	Concrete		Timber	
	compress. (MPa)	tension (MPa)	compress. (MPa)	tension (MPa)
1	-1.35	2.09	-0.69	0.25
2	-4.70	2.49	-1.33	2.69
3	-2.51	1.16	-1.02	1.88

Table 7: *Maximum values of normal stresses in z direction*

Env.	Concrete		Timber	
	compress. (MPa)	tension (MPa)	compress. (MPa)	tension (MPa)
1	-5.68	7.54	-0.90	0.07
2	-7.69	5.79	-0.07	0.91
3	-1.68	2.27	-0.25	0.02

In the case of the warm and dry conditions of Environment 2, the increase in temperature and the decrease in timber moisture caused an increase in compressive stresses on the bottom surface of the concrete in the z-direction, with a value of -7.7 MPa (Figure 12 and Table 7), which is about 14% of the cylinder compressive strength (Table 1).

From all considered environments, the timber slab was subjected to the highest stresses in Environment 2. On the other hand, the tension stress on the top of the timber surface and the compression stress on the bottom surface would reduce the normal stress due to possible future positive bending due to an external load.

It can be concluded that based on the FEM analysis, the normal stresses in the TCC panels caused by the chosen hygrothermal load did not exceed the strength values of the timber or concrete used. On the other hand, standard concrete with a lower value of flexural tensile strength will possibly crack near the glued line and can lead to the failure of the adhesive shear connection.

5.3 SHEAR STRESSES

Figures 15 to 17 show the shear stress diagram on the bottom surface of the concrete since higher values than on the top of the timber were observed (Table 8). According to FEM analysis, the shear stress in the glue line reached the value of the shear strength of the adhesive connection in Environment 2. This may explain the thin cracks in the glue line at the edges of the panels that were observed after the test.

Table 8: *Maximum values of shear stress*

Environment	Concrete (MPa)	Timber (MPa)
1	3.77	1.33
2	4.02	1.51
3	1.99	1.27

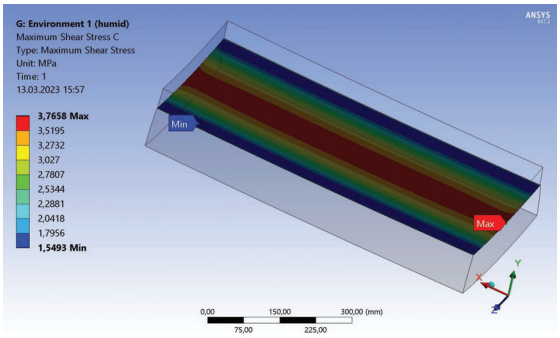

Figure 15: *Humid Environment 1 - Maximum shear stress on the bottom of the concrete*

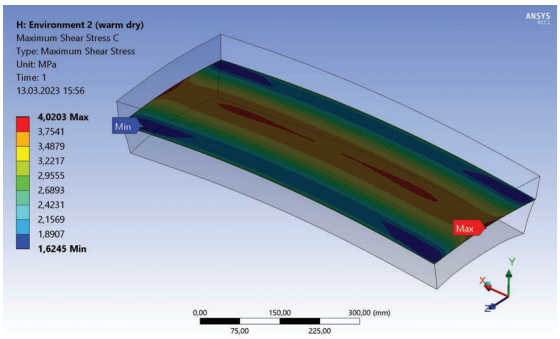

Figure 16: *Warm and dry Environment 2 - Maximum shear stress on the bottom of the concrete*

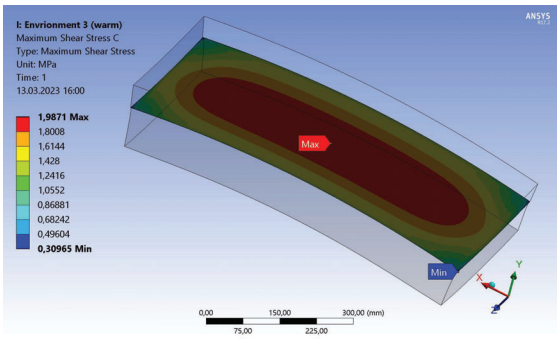

Figure 17: *Warm Environment 3 - Maximum shear stress on the bottom of the concrete*

6 CONCLUSIONS

The hydrothermal stresses near the glue line can limit the use of TCC panels with adhesive shear connections in humid environmental conditions. Therefore, in the experimental analysis, three various environments typical of swimming-pool areas were considered. Based on the measured data, a numerical FEM model was validated and used for the stress evaluation.

From the results, it can conclude that the weakest point of adhesively bonded TCC is the tension stress in the concrete layer. Concrete with a lower value of flexural tensile strength will possibly crack near the glued line and can lead to the failure of the adhesive shear connection. For a humid environment, therefore, high-strength concrete could be more suitable. The shear stress at the edges of the specimens possibly caused the thin cracks in the glued line observed after the test.

The geometrical dimensions of the specimens were relatively small; only fragments of real panels were used in the analysis. But it can assume that the hygrothermal deformations of panels with the same concrete-to-timber ratio cause the same curvature, regardless of the width and length, causing similar normal stresses. On the other hand, the shear stress at the real-size panel edges could possibly be more significant. The size effect will be studied in more depth in future.

Ongoing research focuses on the shear strength differences in the glued line of TCC panel specimens subjected to hygrothermal load over the entire contact surface of the timber and concrete parts of the panels. In addition, further research is still needed to fully comprehend the complex topic of the adhesive connection of TCC, especially in the field of ageing.

ACKNOWLEDGEMENT

This work was supported by the Scientific Grant Agency of the Ministry of Education, Science, Research and Sport of the Slovak Republic and the Slovak Academy of Sciences under Projects VEGA 1/0626/22, VEGA 1/0307/23, and KEGA 030TUKE-4/2022.

REFERENCES

[1] Rodrigues J.N., Dias A., Providência P.: Timber-concrete composite bridges: State-of-the-art review. BioResources 8(4):6630-6649, 2013.

[2] Fragiacomo M., Gregori A., Xue J., Demartino C., Toso M.: Timber-concrete composite bridges: Three case studies. Journal of Traffic and Transportation Engineering (English Edition), 5(6):429-438, 2018.

[3] Naud N., Sorelli L., Salenikovich A., Cuerrier-Auclair S.: Fostering GLULAM-UHPFRC composite structures for multi-storey buildings. Engineering Structures, 188:406-417, 2019.

[4] Estévez-Cimadevila J., Martín-Gutiérrez E., Suárez-Riestra F., Otero-Chans D., Vázquez-Rodríguez J.A.: Timber-concrete composite structural flooring system. Journal of Building Engineering, 49:104078, 2022.

[5] Zhang L., Zhou J., Chui Y.H.: Development of high-performance timber-concrete composite floors with reinforced notched connections. Structures, 39:945-957, 2022.

[6] Pang S.J., Ahn K.S., Jeong S.M., Lee G.C., Kim H.S., Oh J.K.: Prediction of bending performance for a separable CLT-concrete composite slab connected by notch connectors. Journal of Building Engineering, 49:103900, 2022.

[7] Bajzecerová V., Kanócz J., Rovňák M., Kováč M.: Prestressed CLT-concrete composite panels with adhesive shear connection. Journal of Building Engineering, 56: 104785, 2022.

[8] Suárez-Riestra F., Estévez-Cimadevila J., Martín-Gutierrez E., Otero-Chans D.: Perforated shear + reinforcement bar connectors in a timber-concrete composite solution. Analytical and numerical approach. Composites Part B: Engineering, 156:138-147, 2019.

[9] Al-Sammari A.T., Clouston P.L., Breña S.F.: Finite-element analysis and parametric study of perforated steel-plate shear connectors for wood-concrete composites. Journal of Structural Engineering, 144(10):04018191, 2018.

[10] Dias A.M.P.G., Kuhlmann U., Kudla K., Mönch S., Dias A.M.A.: Performance of dowel-type fasteners and notches for hybrid timber structures. Engineering Structures, 171:40-46, 2018.

[11] Nemati Giv A., Fu Q., Yan L., Kasal B.: Interfacial bond behavior of adhesively-bonded timber/cast in situ concrete (wet bond process). Acta Polytechnica CTU Proceedings, 33:398-403, 2022.

[12] Dias A., Schänzlin J., Dietsch P.: Design of timber-concrete composite structures: A state-of-the-art report by COST Action FP1402/ WG 4. Berichte aus dem Bauwesen, Shaker, 2018.

[13] Bajzecerová V., Kanócz J.: Long-term bending test of adhesively bonded timber-concrete composite slabs. In: Advances and Trends in Engineering Sciences and Technologies III, 15-20, 2019.

[14] Eisenhut L., Seim W., Kühlborn S.: Adhesive-bonded timber-concrete composites – Experimental and numerical investigation of hygrothermal effects. Engineering Structures, 125:167-178, 2016.

[15] Tannert T., Endacott B., Brunner M., Vallée T.: Long-term performance of adhesively bonded timber-concrete composites. International Journal of Adhesion and Adhesives, 72:51-61, 2017.

[16] Bajzecerová V., Kanócz J.: The Effect of Environment on Timber-concrete Composite Bridge Deck. Procedia Engineering, 156:32-39, 2016

[17] Ginz A., Seim W.: Moisture-induced internal stress within adhesive-bonded timber-concrete composites. In: *WCTE 2018*, 1-6, 2018.

[18] Jorge L., Dias A., Costa R.: Performance of X-Lam panels in a sports center with an indoor swimming-pool. Journal of Civil Structural Health Monitoring, 5:129-139, 2015.

[19] Bajzecerová V., Kanócz J., Kormaníková E., Karľa V., Orolin P., Vranay F.: Normal Stress Distribution of Timber-Concrete Composite Panels with an Adhesive Shear Connection under Thermal and Humidity Loadings. BioResources, 16(3):4862-4875, 2021.

https://doi.org/10.52202/069179-0419

[20] EN 12390. Testing hardened concrete. European Committee for Standardization, Brussels, Belgium, 2013.
[21] EN 408. Timber structures. Structural timber and glued laminated timber. Determination of some physical and mechanical properties. European Committee for Standardization, Brussels, Belgium, 2013.
[22] Sika, A. G. Product Data Sheet Sikadur®-32 Normal, Sika AG, Baar, Switzerland, 2017.
[23] Ansys Workbench Release 17.2.
[24] Bartolucci B., De Rosa A., Bertolin C., Berto F., Penta F., Siani A. M.: Mechanical properties of the most common European woods: a literature review, Frattura ed Integrità Strutturale, 14(54):249-274, 2020.
[25] Turesson J., Berg S., Björnfot A. et al.: Shear modulus analysis of cross-laminated timber using picture frame tests and finite element simulations. Materials and Structures, 53:112, 2020.